



HAL
open science

Viral vector-mediated Cre recombinase expression in substantia nigra induces lesions of the nigrostriatal pathway associated with perturbations of dopamine-related behaviors and hallmarks of programmed cell death

Sara Rezai Amin, Carole Gruszczynski, Bruno Guiard, Jacques Callebert, Jean-Marie Launay, Franck Louis, Catalina Betancur, Vincent Vialou, Sophie Gautron

► To cite this version:

Sara Rezai Amin, Carole Gruszczynski, Bruno Guiard, Jacques Callebert, Jean-Marie Launay, et al.. Viral vector-mediated Cre recombinase expression in substantia nigra induces lesions of the nigrostriatal pathway associated with perturbations of dopamine-related behaviors and hallmarks of programmed cell death. *Journal of Neurochemistry*, 2019, 150 (3), pp.330-340. 10.1111/jnc.14684 . inserm-02023860

HAL Id: inserm-02023860

<https://inserm.hal.science/inserm-02023860>

Submitted on 18 Feb 2019

HAL is a multi-disciplinary open access archive for the deposit and dissemination of scientific research documents, whether they are published or not. The documents may come from teaching and research institutions in France or abroad, or from public or private research centers.

L'archive ouverte pluridisciplinaire **HAL**, est destinée au dépôt et à la diffusion de documents scientifiques de niveau recherche, publiés ou non, émanant des établissements d'enseignement et de recherche français ou étrangers, des laboratoires publics ou privés.

Viral vector-mediated Cre recombinase expression in substantia nigra induces lesions of the nigrostriatal pathway associated with perturbations of dopamine-related behaviors and hallmarks of programmed cell death

Sara Rezai Amin¹, Carole Gruszczynski¹, Bruno P. Guiard², Jacques Callebert³, Jean-Marie Launay³, Franck Louis¹, Catalina Betancur¹, Vincent Vialou¹, Sophie Gautron¹

1 Sorbonne Université, INSERM, CNRS, Neuroscience Paris Seine, Institut de Biologie Paris Seine, 75005 Paris, France

2 Université de Toulouse, CNRS, Centre de Recherches sur la Cognition Animale, Centre de Biologie Intégrative, 31062 Toulouse, France

3 INSERM U942, Hôpital Lariboisière, Assistance Publique Hôpitaux de Paris, 75010 Paris, France

✉ Corresponding author, sophie.gautron@upmc.fr

Abstract

Cre/loxP recombination is a widely used approach to study gene function *in vivo*, using mice models expressing the Cre recombinase under the control of specific promoters or through viral delivery of Cre-expressing constructs. A profuse literature on transgenic mouse lines points out the deleterious effects of Cre expression in various cell types and tissues, presumably by action at illegitimate loxP-like sites present in the genome. However, most studies reporting the consequences of Cre-lox gene invalidation often omit the adequate controls to exclude potential toxic effects of Cre, compromising the interpretation of data. In this study, we report the anatomical, neurochemical and behavioral consequences in mice of adeno-associated virus (AAV)-mediated Cre expression in the dopaminergic nuclei substantia nigra, at commonly used viral titers (3×10^9 genome copies/0.3 μ L or 2×10^9 genome copies/0.6 μ L). We found that injection of AAV-eGFP-Cre in the SN engendered drastic and reproducible modifications of behavior, with increased basal locomotor activity and impaired locomotor response to cocaine compared to AAV-eGFP-injected controls. Cre expression in the SN induced a massive decrease in neuronal populations of both pars compacta and pars reticulata, and dopamine depletion in the nigrostriatal pathway. This anatomical injury was associated with typical features of programmed cell death, including increase in DNA break markers, evidence of apoptosis and disrupted macroautophagy. These observations underscore the need for careful control of Cre toxicity in the brain and reassessment of previous studies. In addition, our findings suggest that Cre-mediated ablation may constitute an efficient tool to explore the function of specific cell populations and areas in the brain, and the impact of neurodegeneration in these populations.

Key words: Cre recombinase; dopaminergic neurotransmission; programmed cell death; substantia nigra

Abbreviations used: AAV, adeno-associated virus; DA, dopamine; DAT, dopamine transporter; eGFP, enhanced green fluorescent protein; LC3, microtubule-associated protein light chain 3; PD, Parkinson's disease; PMAT, plasma membrane monoamine transporter; PV, parvalbumin; RRID, Research Resource Identifier; SN, substantia nigra; SNc, substantia nigra compacta; SNr, substantia nigra reticulata; TH, tyrosine hydroxylase.

Introduction

The bacteriophage P1 Cre/loxP system has proven a powerful approach to manipulate gene expression *in vivo*, using transgenic mice expressing Cre recombinase under the control of specific promoters or local viral delivery of Cre-encoding constructs. Although this technology has gained universal acceptance, since its discovery several studies have reported non-specific and potentially noxious effects of Cre recombinase in mice in various organs, including the brain. Cre has been incriminated for causing damage in the hematopoietic lineage (Higashi *et al.* 2009), retinal pigment epithelium (Thanos *et al.* 2012), gastric epithelium (Huh *et al.* 2010), and spermatids (Schmidt *et al.* 2000), and inducing cell death in various embryonic tissues (Naiche & Papaioannou 2007) in transgenic mouse models. Cre-induced cardiotoxicity was also established in a mouse line commonly used to generate cardiomyocyte-specific recombination (Bersell *et al.* 2013, Pugach *et al.* 2015). In the brain, behavioral anomalies and flagrant anatomical defects during brain development have been shown to be induced by Cre expression in neuronal progenitors (Forni *et al.* 2006) or the neural crest lineage (Nakajima *et al.* 2013). These detrimental effects have been proposed to be primed by illegitimate Cre action at non-canonical loxP sites within the mouse genome (Schmidt *et al.* 2000, Loonstra *et al.* 2001, Naiche & Papaioannou 2007, Pugach *et al.*), engendering excessive DNA breakage, chromosomal loss, aneuploidy and cell death (Loonstra *et al.* 2001, Huh *et al.* 2010, Zhu *et al.* 2012, Bersell *et al.* 2013, Janbandhu *et al.* 2014) through the improper recruitment of the DNA repair machinery (Sengupta & Harris 2005, Huh *et al.* 2010, Zhu *et al.* 2012). In line with this action at non-canonical loxP sites, Cre-mediated recombination was found responsible for cell death in mouse lines containing multiple tandem copies of transgenes with loxP sites in an inverted configuration (Qiu *et al.* 2011). Taken together, these observations indicate that Cre expressed *in vivo* may produce spurious phenotypes, hampering the analysis of gene function.

Injection of viral vectors mediating Cre expression is another versatile approach often used to study the function of genes in the adult brain (Kaspar *et al.* 2002, Scammell *et al.* 2003, Ahmed *et al.* 2004, Lazarus *et al.* 2011, Tokuoka *et al.* 2011, Krenzer *et al.* 2011, Kopra *et al.* 2017, Bruchas *et al.* 2011, Thanos *et al.* 2012, Lee *et al.* 2013, Yeo & Herbison 2014, Xia *et al.* 2015, Mesic *et al.* 2015, Whitney *et al.* 2016, Foglesong *et al.* 2016, Shen *et al.* 2016). However, the possibility of noxious effects of Cre *per se* in this experimental set-up has been seldom considered. In this study, our attempt to recombine in the brain the gene encoding the plasma membrane monoamine transporter (PMAT) led us to identify unexpected toxic actions of Cre

in the substantia nigra (SN), after adeno-associated virus (AAV) delivery at commonly used titers. AAV-mediated Cre expression in the SN drastically affected behaviors controlled by the basal ganglia circuitry and was associated with a massive decrease in neuronal populations in this brain region and several typical features of programmed cell death.

Material and methods

Animals

Male C57BL/6N wild-type mice (RRID: IMSR_JAX:005304, Charles River, L'Arbresle, France) and *PMAT^{fl/fl}* mice (RRID not registered) were used for the experiments. *PMAT^{fl/fl}* mice were produced by homologous recombination. Briefly, embryonic stem cells harboring a floxed PMAT allele, in which exon 7 has been flanked with loxP sites, were obtained from the Knockout Mice Project (KOMP) repository (*Slc29a4^{tm1a(KOMP)Wtsi}*; UC Davis, CA) and heterozygous mice were generated at the Institut Clinique de la Souris (Illkirch, France). The structure of the floxed PMAT locus was confirmed in *PMAT^{fl/fl}* mice by sequencing (GATC Biotech, Mulhouse, France). *PMAT^{fl/fl}* mice were produced by breeding (CDTA, Orleans, France) and genotyped by polymerase-chain-reaction with primer sets designed to detect the WT and floxed alleles (GAGCCTTGTGTCCTCCTTGTAGGGA/CTAGCCCCTCCCTACATTGCCAA; GTCGCATCCGGAGACATCCACTTTG/TGTTAATCTGCCACAGATCCCGGGC). The study was not pre-registered. Animal care and experiments were conducted in accordance with the European Communities Council Directive for the Care and the Use of Laboratory Animals (2010/63/UE) and approved by the local ethical committee (#5787-2016062207437674).

Adeno-associated virus (AAV) injection

Viral particles expressing eGFP-Cre (AAV2.hSyn.HI.eGFP-Cre.WPRE.SV40) or eGFP (AAV2.hSyn.eGFP.WPRE.bGH) under the control of the human synapsin promoter were obtained from Penn Vector Core (University of Pennsylvania, PA, USA). For AAV injection, eight-week-old male *PMAT^{fl/fl}* (n=36 for AAV-eGFP and 38 for AAV-eGFP-Cre) or WT (n=6 per group) mice were injected with virus expressing either eGFP-Cre or eGFP. Animals were assigned to groups without randomization. Mice were anesthetized with a ketamine-xylazine solution (100 and 10 mg/kg, respectively, i.p.) and the depth of anesthesia was monitored by testing palpebral and pedal reflexes. Purified viruses were injected at a concentration of

3× genome copies/0.3 μL in most experiments; an additional condition, 2×10⁹ genome copies/0.6 μL, was used for comparison in anatomical studies. Viruses were delivered bilaterally over a 3-min period (0.1 μL/min) in the SN at the following coordinates relative to bregma: −3.1 (anterior/posterior), +1.7 (medial/lateral), and −4.4 (dorsal/ventral). The infusion needle was left in situ for 5 min before being slowly withdrawn to prevent backflow. The mice were kept warm under a heat lamp and closely monitored until they had fully recovered, then transferred to their home cage. They were administered an analgesic (10 mg/kg carprofen in drinking water) during 2 days post-operatively. Behavioral, immunohistochemical and neurochemical analyses were performed 8 weeks after surgery and the viral injection sites were confirmed for all mice by examination of GFP fluorescence. A flow chart of the study is presented in Figure 1. Signs of suffering such as vocalizing, loss of mobility, failure to groom and skin lesions, were used as criteria to exclude the animals from further participation in the experiments. No such instance occurred during these experiments. Another prestablished exclusion criterion was injection outside the SN. No animals were excluded from the analyses.

Free-floating immunofluorescence

Mice were anesthetized and perfused intracardially with 4% (wt/vol) paraformaldehyde (PFA)/Sorensen's phosphate buffer (pH 7.4). Brains were removed, post-fixed by immersion in 4% PFA/Sorensen for 48 h and coronal sections (25 μm) were cut on a vibratome and processed for free-floating immunohistochemistry. Sections were preincubated in a blocking buffer containing 0.3% (wt/vol) triton and 4% (wt/vol) bovine serum albumin. Sections were then incubated with primary antibodies against tyrosine hydroxylase (TH, 1/2000, RRID:AB_2201528); dopamine transporter (DAT, 1/2000, RRID:AB_2190413), parvalbumin (PV, 1/15000, RRID:AB_2174013) and S139 phospho-H2AX (1/250, RRID:AB_309864) from Merck Millipore (Billerica, MA, USA); caspase 3 (1/200, RRID:AB_2341188) from Cell Signaling (Danvers, MA, USA); K382 acetyl-p53 (1/250, RRID:AB_2532671) from Thermo Scientific (Rockford, IL, USA); cathepsin D (1/500, RRID:AB_637896) from Santa Cruz Biotechnology (Heidelberg, Germany); and LC3 (LC3B, 1/200, RRID:AB_881433) from Abcam (Cambridge, UK). After washing, sections were incubated with Alexa 555-conjugated secondary antibodies (RRID:AB_162543 and RRID:AB_2536180) from Thermo Scientific. Slides were scanned on a NanoZoomer 2.0-HT (Hamamatsu Photonics, Hamamatsu City, Japan) at 20x resolution. Laser intensity and time of acquisition were set separately for each marker of interest. Positive cells refer to a staining in a cell body clearly above background. The number of cells in SN labeled by TH, PV, pS139 H2AX, AcK382 p53 and LC3, or showing enlarged

lysosomal labeling with cathepsin D was evaluated manually on 2-4 sections for each mouse, at coordinate relative to bregma: -3.1 (anterior/posterior). DAT immunolabeling was quantified with ImageJ software (National Institutes of Health; <http://imagej.nih.gov/ij/>) on four sections per mouse taken from the rostral to caudal regions of the striata, at coordinates relative to bregma: +1.2; +1.0; +0.6 and +0.3 (anterior/posterior). The experimenters were blinded to the treatment of the mice when performing quantification. eGFP and eGFP-Cre expression profiles, which can be distinguished based on their subcellular localization, were evaluated independently.

Determination of monoamine brain content and microdialysis

Determination of monoamine content was performed as previously described (Vialou *et al.* 2008). Briefly, brain structures were dissected from *PMAT^{f/f}* mice injected with AAV2-hSyn-eGFP-Cre or AAV2-hSyn-eGFP, and homogenized in ice-cold buffer (0.1 M acetic acid/10 μ M metabisulfite sodium/10 μ M EDTA/10 μ M ascorbic acid). After centrifugation at 22,000 \times g for 20 minutes at 4°C, the supernatants were collected and filtered through a 10-kDa membrane (Nanosep, Pall Corp., Port Washington, NY) by centrifugation at 7000 \times g. Samples were next assessed for monoamine and metabolite content by ultra high-performance liquid chromatography (UHPLC; UPLC Ultimate 3000, Thermo Scientific) and coulometric detection on a Thermo Scientific Hypersil BDS C 18 column including a Hypersil BDS guard column (analytical conditions: isocratic flow at 0.5 ml/min, oven temperature 35°C, Thermo Scientific phase test, analytical cells potentials 100, 250, 450 and 700 mV). Microdialysis and dopamine (DA) measurements in dorsal striatum were performed as previously described (Maskos *et al.* 2005). Under anesthesia (chloral hydrate, 400 mg/kg, i.p.), mice were stereotaxically implanted with concentric microdialysis probes (active membrane length: 1.5 mm, molecular weight cut-off: 6 kD) in the dorsal striatum, at coordinates relative to bregma: +0.7 (anterior/posterior), \pm 1.8 (medial/lateral), and -4 mm (dorsal/ventral). The following day, mice were connected to a swivel system and the probes connected to a microinjection pump, allowing a continuous perfusion of artificial cerebrospinal fluid (composition: NaCl 147 mM, KCl 3.5 mM, CaCl₂ 1.26 mM, MgCl₂ 1.2 mM, NaH₂PO₄ 1.0 mM, NaHCO₃ 25.0 mM; pH 7.4 \pm 0.2). Dialysate samples were collected every 15 min (flow rate: 1.5 μ L/min) for 3 h, and analyzed for DA content by HPLC coupled to an amperometric detector (VT03; Antec Leyden, Netherlands: limit of sensitivity 0.5 fmol/sample; signal-to-noise ratio = 2) using Chromeleon Lab 7.2 software (Chromeleon Chromatography Data System, Fisher Scientific, Illkirch, Graffenstaden, France). DA basal level was evaluated during 1 h before cocaine injection (30 mg/kg, i.p.).

Behavioral studies

Mice were maintained at 23–25°C on a 12 h light/dark cycle with ad libitum access to food and water. Behavioral studies were performed during the inactive phase (09:00–13:00) with age-matched (16–20 weeks) mice. Behavioral testing was performed sequentially as described in Figure 1. To avoid bias, balanced numbers of AAV-eGFP and AAV eGFP-Cre injected mice were tested in each daily session, and mice of the same age range were tested in each experiment. No specific randomization protocol was used. The experimenters were blinded to the treatment of the mice when performing behavioral assessments. Locomotor activity was assessed in activity chambers (22 x 14 x 11 cm) placed in a rack containing four infrared photobeams located along the long axis. Photobeam interruptions were recorded during 3 h using a computerized tracking system (Imetronic, Bordeaux, France). The open field consisted of a white Plexiglas open-field (42x42 cm) with a luminosity of 35 lux in the center. General locomotor activity in the center and periphery of the open field were scored for 10 min. Time spent in the center zone (20x20 cm) was evaluated as an index of anxiety-related response. For the assessment of anxiety-related behavior in the light-dark box, mice were first placed in the dark compartment then allowed to freely explore both compartments. The time spent and the distance travelled in each compartment were recorded for 5 min by video tracking (Viewpoint, Lyon, France). Locomotor sensitization to cocaine was evaluated in a circular corridor with four infrared captors placed at every 90° angles (Imetronic). Cocaine hydrochloride (10 mg/kg; #1164500, Cooper Industrie, Melun, France) or saline was injected daily during 5 consecutive days (J1-5). Locomotor activity (consecutive interruption of 2 adjacent infrared beams) was recorded after each injection for a period of 30 min.

Statistics

PRISM 6 (GraphPad Software, San Diego, CA, USA) was used for statistical calculations. No sample size calculation was performed. For all the experiments, we used sample sizes that are widely used in the literature. Data normality was evaluated using the Shapiro-Wilks normality test. No outlier test was performed. For cocaine locomotor sensitization, data were analyzed using a two-way analysis of variance (ANOVA) followed by Sidak's post-hoc tests. For all other experiments, data were analyzed using Student's *t*-test if normally distributed. Mann-Whitney test was used when data were not normally distributed i.e., for locomotor activity in the actimeter chamber and the open-field, monoamine HPLC dosage and quantification of TH+ and PV+ cells in the SN. Statistical significance was set at $p < 0.05$.

Results

AAV-mediated Cre expression in the SN alters dopamine-related behaviors and dopaminergic neurotransmission in mice

The initial objective of the study was to characterize the function of PMAT, a low-affinity monoamine transporter expressed in the brain (Vialou *et al.* 2007, Dahlin *et al.* 2007). To this aim, we attempted to invalidate selectively this transporter in the SN, a brain region highly expressing this transporter. AAV-eGFP-Cre or AAV-eGFP viruses, were injected bilaterally in the SN of *PMAT^{fl/fl}* mice at doses classically used for AAV-mediated Cre recombination, 3×10^9 genome copies/0.3 μ L or 2×10^9 genome copies/0.6 μ L (Yu *et al.* 2012, Yeo & Herbison 2014, Shen *et al.* 2016, Kopra *et al.* 2017). eGFP and eGFP-Cre were massively expressed in the SN area of *PMAT^{fl/fl}* mice 2 months after injection, as demonstrated by GFP fluorescence (Fig. 2A), validating the injection site and the efficient expression of Cre. At this time point, *PMAT^{fl/fl}* mice injected with AAV-eGFP-Cre in the SN showed a significant increase in basal locomotor activity compared to *PMAT^{fl/fl}* mice injected with AAV-eGFP (Fig. 2B), coherent with basal ganglia circuitry dysfunction. In parallel, HPLC dosage revealed a selective decrease in intracellular DA and its metabolites in the SN and dorsal striatum of SN AAV-eGFP-Cre injected *PMAT^{fl/fl}* mice (Fig. 2C). In addition, a strong decrease in the extracellular DA level in dorsal striatum was detected in these mice by microdialysis, at basal state and after a cocaine challenge (30 mg/kg, i.p.; Fig. 2D).

To verify whether these alterations were due to PMAT invalidation and exclude eventual off-target effects and Cre toxicity, AAV expressing eGFP-Cre or eGFP were injected in the SN of wild-type (WT) mice in identical conditions to those used in *PMAT^{fl/fl}* mice (Fig. 2A). Unexpectedly, WT mice injected with AAV-eGFP-Cre in the SN presented a clear hyperlocomotor activity compared to eGFP controls (Fig. 2B), similar to that observed in *PMAT^{fl/fl}* mice injected with AAV-eGFP-Cre. For both WT and *PMAT^{fl/fl}* AAV-eGFP-Cre injected mice, this hyperlocomotion was confirmed in the open-field (Fig. 3A). Increased locomotion was accompanied by considerable thigmotaxis, a scanning behavior characterized by the tendency to remain close to the walls of the open-field (Fig. 3A), which has been associated with perturbations of the dopaminergic circuitry (Pogorelov *et al.* 2005, Simon *et al.* 1994). Thigmotaxis was not due to an increase in anxiety level, as shown by the identical performances of mice injected with AAV-eGFP-Cre or with control AAV-eGFP in the light-

dark box (Fig. 3B) and the elevated O-maze (not shown). Mice were next tested for their response to cocaine in a locomotor sensitization paradigm, another behavioral response controlled by dopaminergic signaling. After repeated injections of cocaine (10 mg/kg/day, i.p. for 5 days), AAV-eGFP-Cre injected *PMAT^{fl/fl}* mice exhibited no locomotor sensitization, contrarily to control AAV-eGFP injected *PMAT^{fl/fl}* mice (Fig. 3C). This impairment of locomotor sensitization was also found in AAV-eGFP-Cre injected WT mice, which only responded on the fifth day of cocaine treatment (Fig. 3C).

Thus, AAV-mediated Cre expression in the SN induced basal hyperlocomotion, thigmotaxis and decreased locomotor sensitization to cocaine in both *PMAT^{fl/fl}* and WT mice. These results reveal a selective effect of Cre expression, independent of canonical loxP sites, at concentrations of viral particles similar to those used in previous studies.

AAV-mediated Cre expression in the SN affects the integrity of the nigrostriatal pathway

The consequences of AAV-mediated Cre expression on the anatomical organization of the nigrostriatal dopaminergic pathway were examined by immunohistological staining. Injection of AAV-Cre in the SN of either *PMAT^{fl/fl}* or WT mice decreased considerably the number of dopaminergic neurons in the SN pars compacta (SNc) expressing tyrosine hydroxylase (TH), and of GABAergic neurons of the SN pars reticulata (SNr) expressing parvalbumin (PV), reflecting a decrease in the main neuronal populations of these brain regions (Fig. 4A). This decrease in SNc and SNr populations was found with two different injection conditions, 3×10^9 genome copies/0.3 μ L, the dose used for all experiments (C1), and 1:3 dilution of C1, injected at 2×10^9 genome copies/0.6 μ L (C2). Along with these alterations in neuronal composition in the SN, these mice exhibited a clear loss of dopaminergic projections in the dorsal striatum, as shown by diminished dopamine transporter (DAT) density (Fig. 4B). These anatomical alterations may explain the behavioral and biochemical defects observed after AAV-eGFP-Cre injection in the SN.

AAV-mediated Cre expression in the SN induces an increase in DNA break markers phosphorylated H2XA and K283 acetylated P53

Cre has been postulated to generate DNA breaks, leading to recruitment of the DNA repair machinery to the damaged site, inducing chromosomal alterations and cytotoxicity. To further explicit the nature of the effects of AAV-mediated Cre expression in the SN, we searched in Cre-injected SN of WT mice for evidence of DNA breaks, such as post-translational alterations in histone H2AX and the tumor suppressor P53, both implicated in DNA repair (Lukas *et al.*

2011, Sengupta & Harris 2005). The SN of AAV-eGFP-Cre injected WT mice showed a significant increase in S139 phosphorylated H2AX (Fig. 5A) and K283 acetylated p53 (Fig. 5B), indicating that these two DNA repair factors were strongly activated in the SN of mice receiving AA-eGFP-Cre injection, compared to the SN of mice receiving control AAV-eGFP.

AAV-mediated Cre expression in the SN induces markers of apoptosis and autophagy

The above observations suggest that DNA breakage could prime neurodegeneration in the SN of AAV-eGFP-Cre injected mice. In particular, failure to control DNA damage and the inappropriate engagement of the DNA repair machinery might activate cell death processes such as apoptosis and autophagy, both implicated in neurodegeneration in Parkinson's disease (PD) (Dauer & Przedborski 2003, Venderova & Park 2012, Michel *et al.* 2016). Earlier studies suggested that the p53 DNA damage-induced pathway could be implicated in Cre-mediated apoptosis following the action of the recombinase at loxP sites (Zhu *et al.* 2012). Strikingly, Ser 139 phosphorylated H2AX in the SN of AAV-eGFP-Cre injected mice showed a peculiar distribution at the nuclear periphery inside the nuclear envelope (Fig. 5A), a typical pattern reflecting apoptosis (Solier & Pommier 2009). We thus next explored whether caspase 3, a main actor of apoptosis (Taylor *et al.* 2008), was activated in AAV-eGFP-Cre injected mice. Low and comparable immunofluorescent labeling of D175-cleaved caspase 3 was detected in the SN of AAV-eGFP-Cre and AAV-eGFP injected mice, contrasting with the positive labeling on the needle tracts in the cortex of both groups (Fig. 5C), suggesting that caspase 3-dependent apoptosis was not implicated in Cre-mediated toxicity in this brain region. Lastly, we explored whether perturbations of autophagy processes were also associated with Cre-induced cell death in the SN. As autophagy is intimately linked with lysosomal function (Scrivero *et al.* 2018), the consequences of Cre expression were further evaluated by assessing immunolabeling of the lysosomal enzyme cathepsin D and of LC3, a component of the autophagy machinery. Significant alterations of the distribution of cathepsin D and LC3 labeling were induced by AAV-GFP-Cre injection compared to control AAV-GFP. The number of cells showing normalized lysosomes labeled with cathepsin D was decreased while the labeling was redistributed into large compartments (Fig. 5D, upper panels), indicative of autolysosome accumulation (Crews *et al.* 2010). Additionally, while LC3 labeling did not appear notably altered in the whole SN, this labeling was significantly decreased in eGFP-Cre expressing cells compared to eGFP expressing cells (Fig. 5D, lower panels). Diminished LC3 expression has been also associated with prolonged autophagy and fusion of autophagosomes with lysosomes (Kimura

et al. 2007), further supporting the importance of perturbations of autophagy processes in Cre-induced toxicity in the SN.

Discussion

In this study, we found that local AAV-mediated Cre expression in the SN can potently damage the nigrostriatal dopaminergic pathway, leading to an original anatomical and functional phenotype sharing some similarities with neurodegenerative diseases and models of dopaminergic degeneration. Our report is to our knowledge the first demonstration of AAV-Cre mediated toxicity in the brain, identified as such, at commonly used doses of viral particles. The damaging effects observed were penetrating, with dramatic wide-ranging functional consequences. They did not require the presence of canonical loxP sites, as they occurred in wild-type mice, and nor could they be attributed to virus injection, since they were revealed by comparison with AAV-eGFP controls. **Further investigations using an inactive mutant Cre construct should prove useful to sort out the relative contribution of Cre recombinase per se and its coupling to eGFP in these effects.**

Compared with known neurodegeneration models (Dauer & Przedborski 2003), Cre-mediated toxicity appeared surprisingly efficient and reproducible, with massive decreases in neuronal populations in both SNc and SNr. The overall phenotype induced by Cre expression in the SN, associating lasting hyperlocomotor activity with DA depletion, was fundamentally compatible with current knowledge of basal ganglia circuitry. As expected, SNc damage led to a decrease in intracellular DA content in the SN and striatum, density of dopaminergic projections in the striatum, and extracellular DA in this brain area at basal state and after cocaine challenge. These neurochemical alterations can fully account for the impaired response to acute and repeated cocaine injection in Cre-injected mice (Giros *et al.* 1996). This anatomical and functional phenotype shares some resemblance with PD (Dauer & Przedborski 2003) and animal models of the disease (Jagmag *et al.* 2015), which show degeneration of the nigrostriatal DA pathway and striatal DA deficiency, responsible for the sensory-motor symptoms in PD patients (Dauer & Przedborski 2003). However, contrarily to PD pathophysiology, Cre expression in the SN also induced massive cellular damage in the SNr, leading to increased basal locomotor activity in mice. The activity of the SNr, a major hub of the basal ganglia circuitry, tonically inhibits pre-motor structures in the thalamus and brainstem, and constricts motor activity (Deniau *et al.* 2007). Hence, hyperlocomotor activity in Cre-injected mice was

most probably a consequence of a disinhibition of the thalamocortical pathway due to SNr damage (Baumeister *et al.* 1988, Olanas *et al.* 1978).

Our study reveals the involvement of basic cellular processes previously implicated in Cre toxicity. In-depth studies in mammalian cells culture have demonstrated that Cre activity can induce growth inhibition and extensive chromosomal alterations, such as aneuploidy and sister chromatid exchange (Loonstra *et al.* 2001). These genotoxic effects involve the action of Cre at endogenous degenerate loxP sites (Thyagarajan *et al.* 2000), generating extremely rapidly double strand breaks, damaging DNA beyond repair, and recruiting the tumor suppressor p53 which regulates almost all DNA repair processes (Sengupta & Harris 2005, Zhu *et al.* 2012). Several hundreds of these loxP-like sites have been identified in the mouse genome, and their role in the detrimental effects of Cre recombinase *in vivo* has been established in various models (Schmidt *et al.* 2000, Loonstra *et al.* 2001, Qiu *et al.* 2011, Pugach *et al.* 2015). In agreement with these mechanisms, Cre-injected SN shows pronounced increases in the DNA break markers phospho-H2XA and acetylated p53. By its central role at the intersection of DNA repair and cell cycle pathways, p53 is an important regulator of programmed cell death (Sengupta & Harris 2005), controlling apoptosis and autophagy (Maiuri *et al.* 2010). Defective DNA repair has been reported for a number of neurodegenerative disorders (Madabhushi *et al.* 2014). Recent studies also underscore the importance of programmed cell death in PD (Venderova & Park 2012), and p53 levels have been found increased in the brain of patients (da Costa & Checler 2010, de la Monte *et al.* 1998). Remarkably, both apoptotic and autophagic cell death appears to be induced by Cre expression in the SN. The presence of apoptotic rings (Solier & Pommier 2009) without caspase 3 activation supports a role of a caspase-independent apoptosis pathway in Cre-mediated toxicity, such as the intrinsic pathway involving apoptosis-inducing factor 1 (Daugas *et al.* 2000). Enlarged lysosomal compartments and LC3 disappearance reflect an increase in the formation of autolysosomes, a hallmark of impaired autophagy found in several neurological disorders (Crews *et al.* 2010, Yang *et al.* 2011, Tanik *et al.* 2013).

Our results along with reports of Cre toxicity in transgenic mice emphasize the importance of appropriate controls for Cre effects, seldom included in studies implicating Cre-mediated recombination. AAV-mediated Cre recombination is a common approach for gene function study in the brain including in the SN (Tokuoka *et al.* 2011, Yu *et al.* 2012), with viral titers often comparable to those used in our study (Yu *et al.* 2012, Yeo & Herbison 2014, Shen *et al.* 2016, Kopra *et al.* 2017), but the local effects of Cre expression have been poorly investigated. Preserving an appropriate balance between recombination of the target gene and toxicity is an

important pitfall in studies using Cre recombinase. Cre toxicity has been shown to increase in some cases in a time-dependent manner along with its accumulation (Pugach et al. 2015), suggesting that curbing Cre expression in the target area could limit damage. On the other hand, reduction of Cre expression was shown to compromise recombination as well (Loonstra et al. 2001, Naiche & Papaioannou 2007). **Further investigation using a recombinant activity-deficient Cre construct may allow to dissect more finely the contribution of Cre whether or not coupled with GFP in future studies.**

Additional studies beyond the scope of the present report are required to identify the appropriate conditions and virus doses allowing efficient recombination in a given brain area while avoiding cellular damage. In this context, Cre with improved accuracy (Eroshenko & Church 2013) or delivered by constructs allowing self-excision (Silver & Livingston 2001), may offer promising alternatives to circumvent these obstacles. Conversely, Cre has been proposed previously as an efficient tool to carry out conditional cell ablation (Grégoire & Kmita 2008, Qiu et al. 2011). These cytotoxic effects could be used to generate local lesion models and eventually be applied to other brain regions provided they show the same sensitivity than the SN.

To conclude, these findings underscore the potential neurotoxic effects of Cre recombinase in the brain that may go undetected unless specifically sought for, with major functional consequences. These damaging effects, which implicate cellular mechanisms common to neurodegenerative diseases such as deregulation of DNA repair processes, recruitment of p53 and induction of programmed cell death, may be exploited in the future to generate region or cell-specific models of neurodegeneration.

Acknowledgements and conflict of interest disclosure

We thank F. Machulka for expert assistance with animal care. This work was supported by INSERM, CNRS, Sorbonne Université and the Agence Nationale de la Recherche (ANR-13-SAMENTA-0003-01). S.R. was a recipient of a fellowship from the French Ministry for Research. This work is dedicated to the memory of Dr. Marie-Pascale Martres. The authors declare no conflict of interest.

References

- Ahmed, B. Y., Chakravarthy, S., Eggers, R. et al. (2004) Efficient delivery of Cre-recombinase to neurons in vivo and stable transduction of neurons using adeno-associated and lentiviral vectors. *BMC Neurosci.*, **5**, 4.
- Baumeister, A. A., Hawkins, M. F., Anderson-Moore, L. L., Anticich, T. G., Higgins, T. D. and Griffin, P. (1988) Effects of bilateral injection of GABA into the substantia nigra on spontaneous behavior and measures of analgesia. *Neuropharmacology*, **27**, 817-821.
- Bersell, K., Choudhury, S., Mollova, M., Polizzotti, B. D., Ganapathy, B., Walsh, S., Wadugu, B., Arab, S. and Kuhn, B. (2013) Moderate and high amounts of tamoxifen in alphaMHC-MerCreMer mice induce a DNA damage response, leading to heart failure and death. *Dis. Model Mech.*, **6**, 1459-1469.
- Bruchas, M. R., Schindler, A. G., Shankar, H. et al. (2011) Selective p38alpha MAPK deletion in serotonergic neurons produces stress resilience in models of depression and addiction. *Neuron*, **71**, 498-511.
- Crews, L., Spencer, B., Desplats, P. et al. (2010) Selective molecular alterations in the autophagy pathway in patients with Lewy body disease and in models of alpha-synucleinopathy. *PLoS One*, **5**, e9313.
- da Costa, C. A. and Checler, F. (2010) A novel parkin-mediated transcriptional function links p53 to familial Parkinson's disease. *Cell Cycle*, **9**, 16-17.
- Dahlin, A., Xia, L., Kong, W., Hevner, R. and Wang, J. (2007) Expression and immunolocalization of the plasma membrane monoamine transporter in the brain. *Neuroscience*, **146**, 1193-1211.
- Dauer, W. and Przedborski, S. (2003) Parkinson's disease: mechanisms and models. *Neuron*, **39**, 889-909.
- Daugas, E., Susin, S. A., Zamzami, N. et al. (2000) Mitochondrio-nuclear translocation of AIF in apoptosis and necrosis. *FASEB J.*, **14**, 729-739.
- de la Monte, S. M., Sohn, Y. K., Ganju, N. and Wands, J. R. (1998) P53- and CD95-associated apoptosis in neurodegenerative diseases. *Lab. Invest.*, **78**, 401-411.
- Deniau, J. M., Mailly, P., Maurice, N. and Charpier, S. (2007) The pars reticulata of the substantia nigra: a window to basal ganglia output. *Prog. Brain Res.*, **160**, 151-172.
- Eroshenko, N. and Church, G. M. (2013) Mutants of Cre recombinase with improved accuracy. *Nat. Commun.*, **4**, 2509.

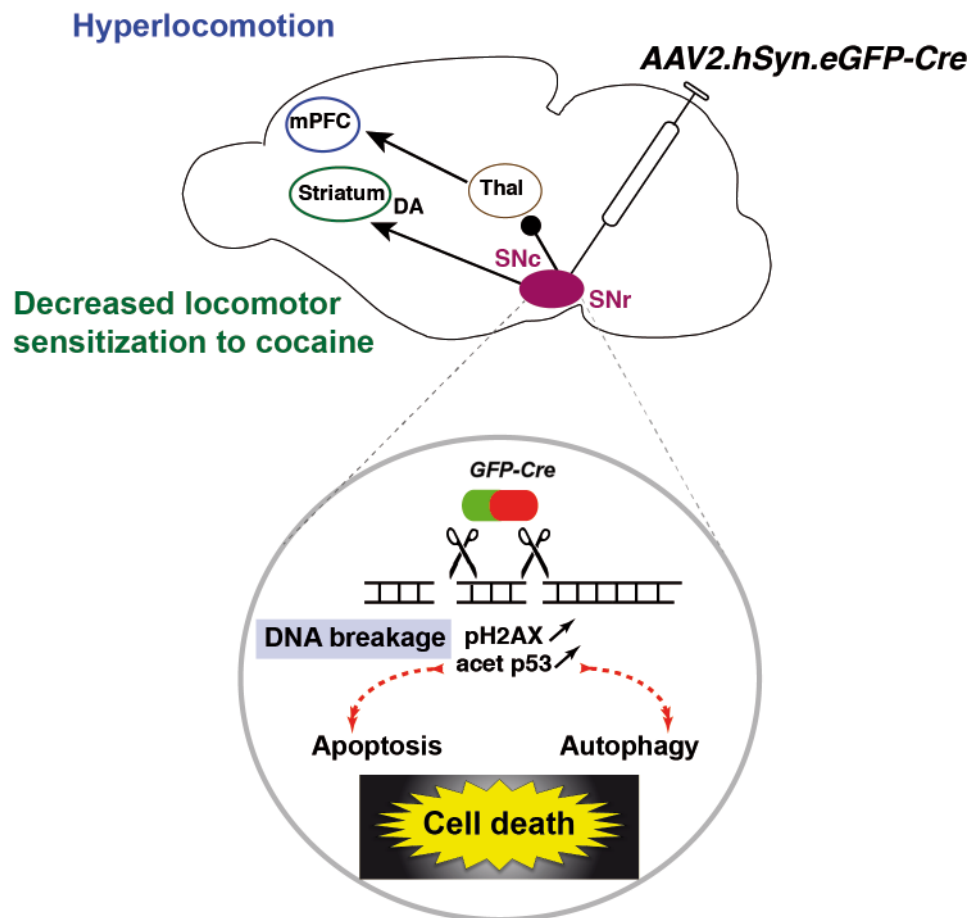
- Foglesong, G. D., Huang, W., Liu, X., Slater, A. M., Siu, J., Yildiz, V., Salton, S. R. J. and Cao, L. (2016) Role of Hypothalamic VGF in Energy Balance and Metabolic Adaption to Environmental Enrichment in Mice. *Endocrinology*, **157**, 983-996.
- Forni, P. E., Scuoppo, C., Imayoshi, I. et al. (2006) High levels of Cre expression in neuronal progenitors cause defects in brain development leading to microencephaly and hydrocephaly. *J. Neurosci.*, **26**, 9593-9602.
- Giros, B., Jaber, M., Jones, S. R., Wightman, R. M. and Caron, M. G. (1996) Hyperlocomotion and indifference to cocaine and amphetamine in mice lacking the dopamine transporter. *Nature*, **379**, 606-612.
- Grégoire, D. and Kmita, M. (2008) Recombination between inverted loxP sites is cytotoxic for proliferating cells and provides a simple tool for conditional cell ablation. *Proc. Natl. Acad. Sci. U S A*, **105**, 14492-14496.
- Higashi, A. Y., Ikawa, T., Muramatsu, M. et al. (2009) Direct hematological toxicity and illegitimate chromosomal recombination caused by the systemic activation of CreERT2. *J. Immunol.*, **182**, 5633-5640.
- Huh, W. J., Mysorekar, I. U. and Mills, J. C. (2010) Inducible activation of Cre recombinase in adult mice causes gastric epithelial atrophy, metaplasia, and regenerative changes in the absence of "floxed" alleles. *Am. J. Physiol. Gastrointest. Liver Physiol.*, **299**, G368-380.
- Jagmag, S. A., Tripathi, N., Shukla, S. D., Maiti, S. and Khurana, S. (2015) Evaluation of Models of Parkinson's Disease. *Front. Neurosci.*, **9**, 503.
- Janbandhu, V. C., Moik, D. and Fässler, R. (2014) Cre recombinase induces DNA damage and tetraploidy in the absence of loxP sites. *Cell Cycle* **13**, 462-470.
- Kaspar, B. K., Vissel, B., Bengoechea, T. et al. (2002) Adeno-associated virus effectively mediates conditional gene modification in the brain. *Proc. Natl. Acad. Sci. U S A*, **99**, 2320-2325.
- Kimura, S., Noda, T. and Yoshimori, T. (2007) Dissection of the autophagosome maturation process by a novel reporter protein, tandem fluorescent-tagged LC3. *Autophagy*, **3**, 452-460.
- Kopra, J. J., Panhelainen, A., Af Bjerkén, S. et al. (2017) Dampened Amphetamine-Stimulated Behavior and Altered Dopamine Transporter Function in the Absence of Brain GDNF. *J. Neurosci.*, **37**, 1581-1590.
- Krenzer, M., Anaclet, C., Vetrivelan, R., Wang, N., Vong, L., Lowell, B. B., Fuller, P. M. and Lu, J. (2011) Brainstem and spinal cord circuitry regulating REM sleep and muscle atonia. *PloS One*, **6**, e24998.

- Lazarus, M., Shen, H.-Y., Cherasse, Y. et al. (2011) Arousal effect of caffeine depends on adenosine A2A receptors in the shell of the nucleus accumbens. *J. Neurosci.*, **31**, 10067-10075.
- Lee, N., Batt, M. K., Cronier, B. A. et al. (2013) Ciliary neurotrophic factor receptor regulation of adult forebrain neurogenesis. *J. Neurosci.*, **33**, 1241-1258.
- Loonstra, A., Vooijs, M., Beverloo, H. B., Allak, B. A., van Drunen, E., Kanaar, R., Berns, A. and Jonkers, J. (2001) Growth inhibition and DNA damage induced by Cre recombinase in mammalian cells. *Proc. Natl. Acad. Sci. U S A*, **98**, 9209-9214.
- Lukas, J., Lukas, C. and Bartek, J. (2011) More than just a focus: The chromatin response to DNA damage and its role in genome integrity maintenance. *Nat. Cell. Biol.*, **13**, 1161-1169.
- Madabhushi, R., Pan, L. and Tsai, L. H. (2014) DNA damage and its links to neurodegeneration. *Neuron*, **83**, 266-282.
- Maiuri, M. C., Galluzzi, L., Morselli, E., Kepp, O., Malik, S. A. and Kroemer, G. (2010) Autophagy regulation by p53. *Curr. Opin. Cell. Biol.*, **22**, 181-185.
- Maskos, U., Molles, B. E., Pons, S. et al. (2005) Nicotine reinforcement and cognition restored by targeted expression of nicotinic receptors. *Nature*, **436**, 103-107.
- Mesic, I., Guzman, Y. F., Guedea, A. L., Jovasevic, V., Corcoran, K. A., Leaderbrand, K., Nishimori, K., Contractor, A. and Radulovic, J. (2015) Double Dissociation of the Roles of Metabotropic Glutamate Receptor 5 and Oxytocin Receptor in Discrete Social Behaviors. *Neuropsychopharmacology*, **40**, 2337-2346.
- Michel, P. P., Hirsch, E. C. and Hunot, S. (2016) Understanding Dopaminergic Cell Death Pathways in Parkinson Disease. *Neuron*, **90**, 675-691.
- Naiche, L. A. and Papaioannou, V. E. (2007) Cre activity causes widespread apoptosis and lethal anemia during embryonic development. *Genesis*, **45**, 768-775.
- Nakajima, M., Mori, H., Nishikawa, C., Tsuruta, M., Okuyama, S. and Furukawa, Y. (2013) Psychiatric disorder-related abnormal behavior and habenulointerpeduncular pathway defects in Wnt1-cre and Wnt1-GAL4 double transgenic mice. *J. Neurochem.*, **124**, 241-249.
- Olianas, M. C., De Montis, G. M., Concu, A., Tagliamonte, A. and di Chiara, G. (1978) Intranigral kainic acid: evidence for nigral non-dopaminergic neurons controlling posture and behavior in a manner opposite to the dopaminergic ones. *Eur. J. Pharmacol.*, **49**, 223-232.

- Pogorelov, V. M., Rodriguiz, R. M., Insko, M. L., Caron, M. G. and Wetsel, W. C. (2005) Novelty seeking and stereotypic activation of behavior in mice with disruption of the *Dat1* gene. *Neuropsychopharmacology*, **30**, 1818-1831.
- Pugach, E. K., Richmond, P. A., Azofeifa, J. G., Dowell, R. D. and Leinwand, L. A. (2015) Prolonged Cre expression driven by the α -myosin heavy chain promoter can be cardiotoxic. *J. Mol. Cell. Cardiol.*, **86**, 54-61.
- Qiu, L., Rivera-Pérez, J. A. and Xu, Z. (2011) A non-specific effect associated with conditional transgene expression based on Cre-loxP strategy in mice. *PloS One*, **6**, e18778.
- Scammell, T. E., Arrigoni, E., Thompson, M. A., Ronan, P. J., Saper, C. B. and Greene, R. W. (2003) Focal deletion of the adenosine A1 receptor in adult mice using an adeno-associated viral vector. *J. Neurosci.*, **23**, 5762-5770.
- Schmidt, E. E., Taylor, D. S., Prigge, J. R., Barnett, S. and Capecchi, M. R. (2000) Illegitimate Cre-dependent chromosome rearrangements in transgenic mouse spermatids. *Proc. Natl. Acad. Sci. U S A*, **97**, 13702-13707.
- Scrivo, A., Bourdenx, M., Pampliega, O. and Cuervo, A. M. (2018) Selective autophagy as a potential therapeutic target for neurodegenerative disorders. *Lancet Neurol.*, **17**, 802-815.
- Sengupta, S. and Harris, C. C. (2005) p53: traffic cop at the crossroads of DNA repair and recombination. *Nature Rev. Mol. Cell Biol.*, **6**, 44-55.
- Shen, M., Jiang, C., Liu, P., Wang, F. and Ma, L. (2016) Mesolimbic leptin signaling negatively regulates cocaine-conditioned reward. *Transl. Psychiatry*, **6**, e972.
- Silver, D. P. and Livingston, D. M. (2001) Self-excising retroviral vectors encoding the Cre recombinase overcome Cre-mediated cellular toxicity. *Mol. Cell*, **8**, 233-243.
- Simon, P., Dupuis, R. and Costentin, J. (1994) Thigmotaxis as an index of anxiety in mice. Influence of dopaminergic transmissions. *Behav. Brain Res.*, **61**, 59-64.
- Solier, S. and Pommier, Y. (2009) The apoptotic ring: a novel entity with phosphorylated histones H2AX and H2B and activated DNA damage response kinases. *Cell Cycle*, **8**, 1853-1859.
- Tanik, S. A., Schultheiss, C. E., Volpicelli-Daley, L. A., Brunden, K. R. and Lee, V. M. (2013) Lewy body-like alpha-synuclein aggregates resist degradation and impair macroautophagy. *J. Biol. Chem.*, **288**, 15194-15210.
- Taylor, R. C., Cullen, S. P. and Martin, S. J. (2008) Apoptosis: controlled demolition at the cellular level. *Nat. Rev. Mol. Cell Biol.*, **9**, 231-241.
- Thanos, A., Morizane, Y., Murakami, Y. et al. (2012) Evidence for baseline retinal pigment epithelium pathology in the Trp1-Cre mouse. *Am. J. Pathol.*, **180**, 1917-1927.

- Thyagarajan, B., Guimarães, M. J., Groth, A. C. and Calos, M. P. (2000) Mammalian genomes contain active recombinase recognition sites. *Gene*, **244**, 47-54.
- Tokuoka, H., Muramatsu, S.-i., Sumi-Ichinose, C., Sakane, H., Kojima, M., Aso, Y., Nomura, T., Metzger, D. and Ichinose, H. (2011) Compensatory regulation of dopamine after ablation of the tyrosine hydroxylase gene in the nigrostriatal projection. *J. Biol. Chem.*, **286**, 43549-43558.
- Venderova, K. and Park, D. S. (2012) Programmed cell death in Parkinson's disease. *Cold Spring Harb. Perspect. Med.*, **2**.
- Vialou, V., Balasse, L., Callebert, J., Launay, J. M., Giros, B. and Gautron, S. (2008) Altered aminergic neurotransmission in the brain of organic cation transporter 3-deficient mice. *J Neurochem*, **106**, 1471-1482.
- Vialou, V., Balasse, L., Dumas, S., Giros, B. and Gautron, S. (2007) Neurochemical characterization of pathways expressing plasma membrane monoamine transporter in the rat brain. *Neuroscience*, **144**, 616-622.
- Whitney, M. S., Shemery, A. M., Yaw, A. M., Donovan, L. J., Glass, J. D. and Deneris, E. S. (2016) Adult Brain Serotonin Deficiency Causes Hyperactivity, Circadian Disruption, and Elimination of Siestas. *J. Neurosci.*, **36**, 9828-9842.
- Xia, H., de Queiroz, T. M., Sriramula, S., Feng, Y., Johnson, T., Mungrue, I. N. and Lazartigues, E. (2015) Brain ACE2 overexpression reduces DOCA-salt hypertension independently of endoplasmic reticulum stress. *Am. J. Physiol. Reg. Integr. Comp. Physiol.*, **308**, R370-378.
- Yang, D. S., Stavrides, P., Mohan, P. S. et al. (2011) Reversal of autophagy dysfunction in the TgCRND8 mouse model of Alzheimer's disease ameliorates amyloid pathologies and memory deficits. *Brain*, **134**, 258-277.
- Yeo, S.-H. and Herbison, A. E. (2014) Estrogen-negative feedback and estrous cyclicity are critically dependent upon estrogen receptor- α expression in the arcuate nucleus of adult female mice. *Endocrinology*, **155**, 2986-2995.
- Yu, S.-J., Airavaara, M., Shen, H., Chou, J., Harvey, B. K. and Wang, Y. (2012) Suppression of endogenous PPAR γ increases vulnerability to methamphetamine-induced injury in mouse nigrostriatal dopaminergic pathway. *Psychopharmacology*, **221**, 479-492.
- Zhu, J., Nguyen, M.-T., Nakamura, E., Yang, J. and Mackem, S. (2012) Cre-mediated recombination can induce apoptosis in vivo by activating the p53 DNA damage-induced pathway. *Genesis*, **50**, 102-111.

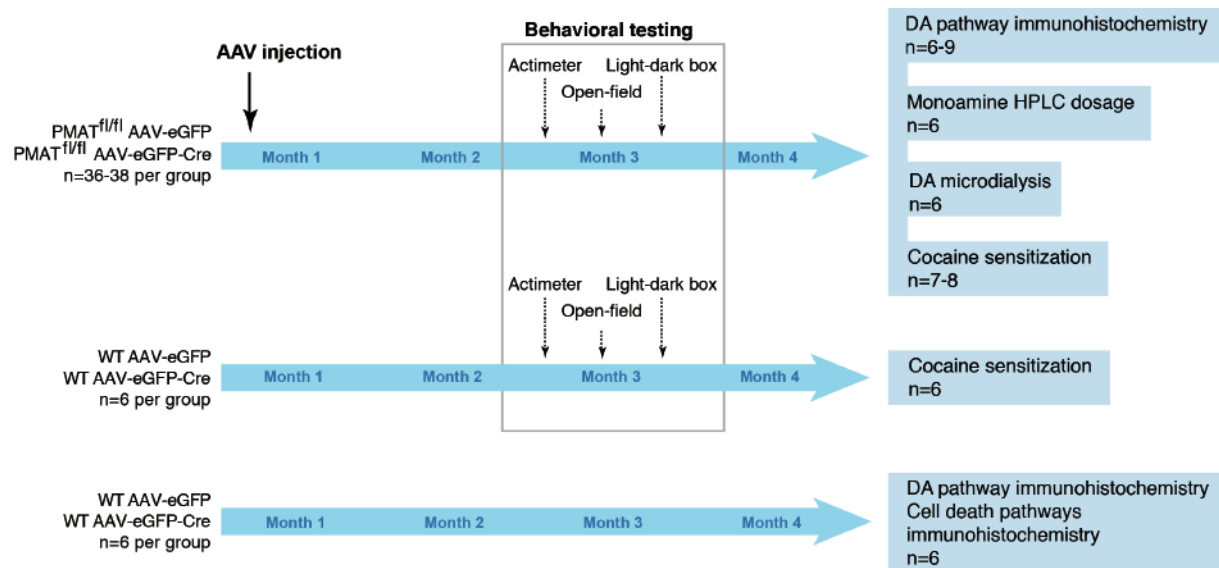
Graphical abstract



Cre/loxP recombination is a widely used approach to study gene function in vivo, using mice models expressing the Cre recombinase under the control of specific promoters or through viral delivery of Cre-expressing constructs. Our experiments show that AAV-mediated Cre recombinase expression in the substantia nigra (SN) provokes lesions of the SN pars compacta and reticulata and perturbations of dopamine-related behaviors by inducing DNA breakage, increased apoptosis and perturbation of autophagy. These observations underscore the need for careful control of Cre toxicity when using this tool to study gene function in the brain.

Figures

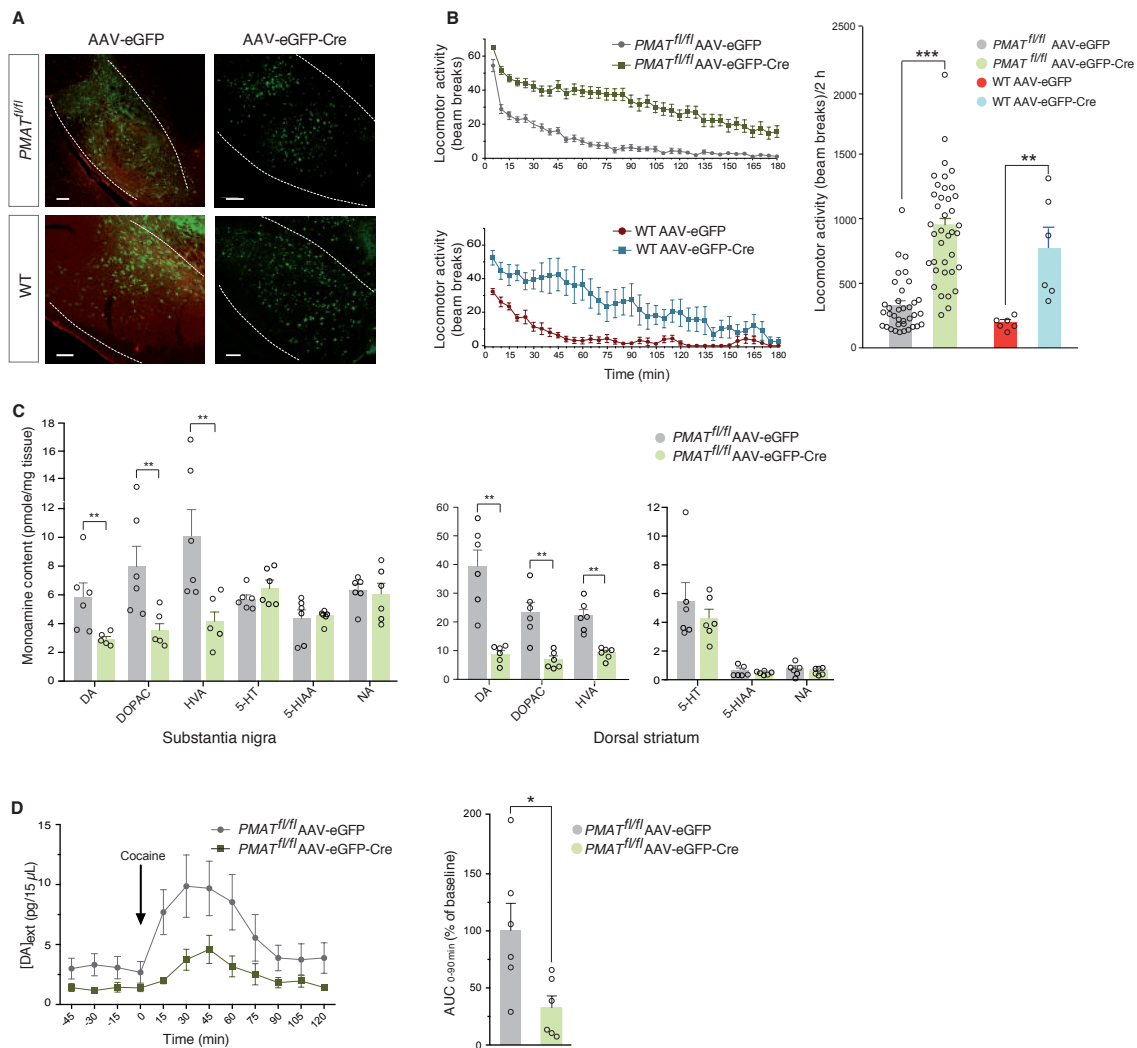
Figure 1



Flowchart of the experimental procedures.

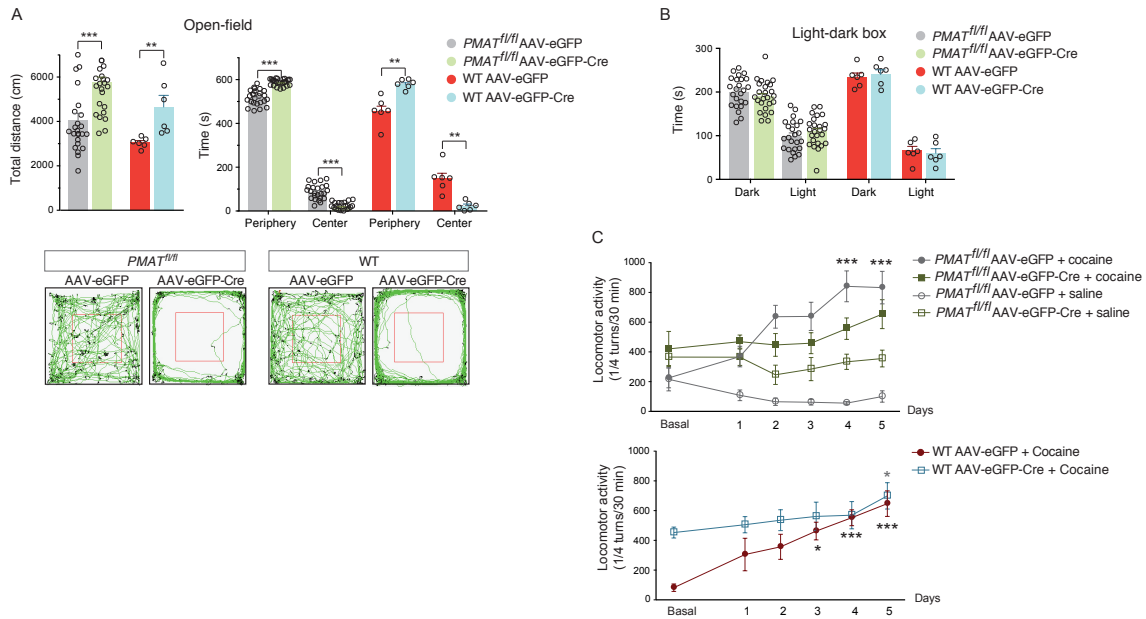
Viral particles expressing eGFP-Cre or eGFP were injected into eight-week-old male *PMAT^{fl/fl}* or WT mice. Behavioral, immunohistochemical and neurochemical analyses were performed between 8 to 10 weeks after AAV injection. After behavioral testing, 2/3 of the *PMAT^{fl/fl}* mice were submitted to four distinct types of experiments. The viral injection sites were confirmed for all *PMAT^{fl/fl}* or WT mice except those submitted to microdialysis and HPLC dosage, by examination of GFP fluorescence; *n*=number of animals in experimental groups.

Figure 2



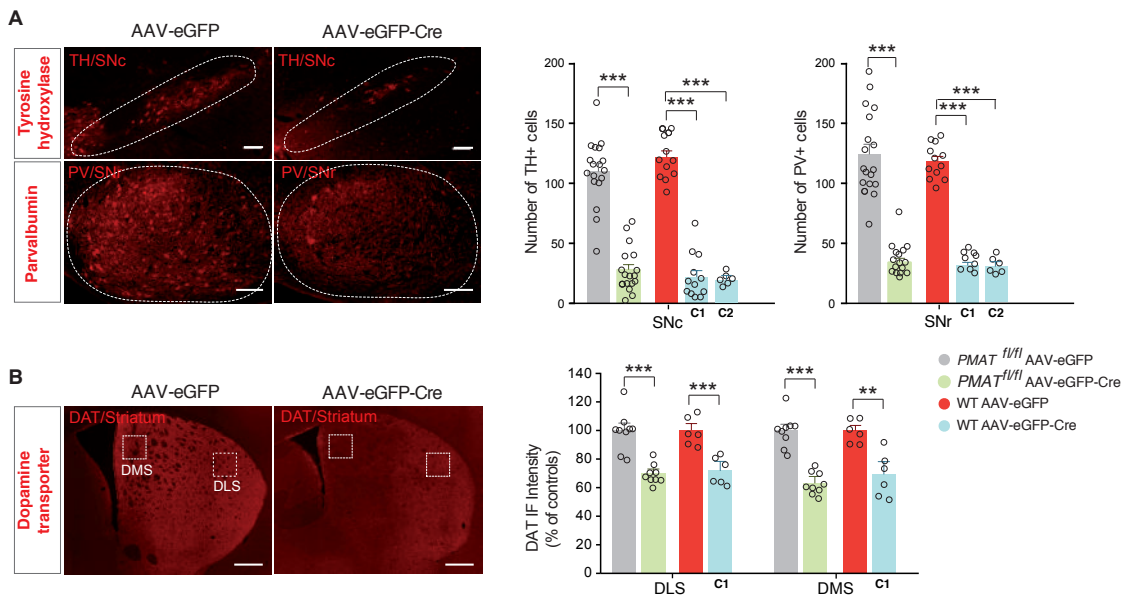
Alterations of dopamine-related behaviors and dopaminergic signaling induced by AAV-mediated Cre expression in the SN of mice. (A) GFP fluorescence validated expression of AAV-eGFP and AAV-eGFP-Cre, and accuracy of injection site in the SN; representative images of *PMAT^{fl/fl}* (top) and WT mice (bottom). SNc dopaminergic neurons are labeled with tyrosine hydroxylase in AAV-GFP-injected mice. Scale bars: 100 μ m. (B) AAV-mediated Cre expression in the SN of *PMAT^{fl/fl}* mice (n=36-38 per group) and WT mice (n=6 per group) increased locomotor activity in the actimeter chamber, evaluated by the number of photobeam breaks measured in 5-min intervals during 3 h (left) and integrated over 2 h (right). Mann-Whitney test, unpaired, ** p<0.01, *** p<0.001. (C) HPLC dosage revealed a selective decrease in intratissular DA and its metabolites in the SN and dorsal striatum of AAV-eGFP-Cre-injected *PMAT^{fl/fl}* mice compared to AAV-eGFP-injected *PMAT^{fl/fl}* mice (n=6 mice per group). Mann-Whitney test, unpaired, ** p<0.01. (D) Microdialysis analysis showed a strong decrease in extracellular DA level in the dorsal striatum after cocaine injection in AAV-eGFP Cre-injected *PMAT^{fl/fl}* mice compared to AAV-eGFP *PMAT^{fl/fl}* mice (n=6 mice per group). Student t-test, unpaired, * p<0.05. Values are given as mean \pm s.e.m; individual points are also shown for bars.

Figure 3.



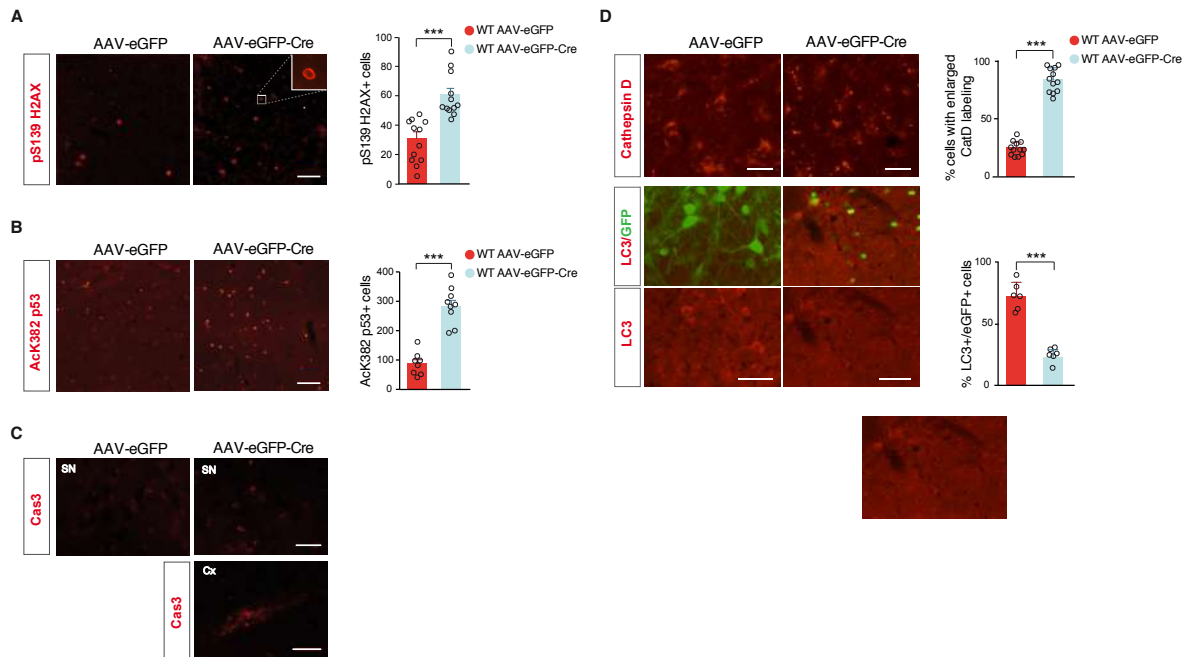
High thigmotaxis and impaired response to cocaine induced by AAV-mediated Cre expression in the SN of mice. (A) AAV-mediated Cre expression in the SN of *PMAT^{fl/fl}* mice (n=21-23 per group) and WT mice (n=6 per group) increased locomotor activity and decreased time spent in the center of the open field (top), reflecting strong thigmotaxis (bottom). Mann-Whitney test, unpaired, ** p<0.01, *** p<0.001. (B) AAV-mediated Cre expression in the SN of *PMAT^{fl/fl}* mice (n=24-25 per group) and WT mice (n=6 per group) did not modify anxiety level in the light dark box). (C) AAV-mediated Cre expression in the SN of *PMAT^{fl/fl}* and WT mice disrupted locomotor sensitization to cocaine (10 mg/kg). Two-way analysis of variance (ANOVA) revealed main significant effects of cocaine treatment ($F_{1,14} = 5.640$; $P = 0.0324$), and day of cocaine treatment ($F_{4,56} = 5.617$; $P = 0.0007$) for *PMAT^{fl/fl}* mice (n=7-8 per group), and of day of cocaine treatment ($F_{5,50} = 20.52$; $P < 0.0001$) and day of treatment/AAV type interaction ($F_{5,50} = 4.338$; $P = 0.0023$) for WT mice (n=6 per group). Over time, Sidak's post-hoc test showed stronger locomotor sensitization for AAV-eGFP-injected mice than for AAV-eGFP-Cre-injected mice (* p<0.05, ** p<0.01, *** p<0.001, compared to day 1). Values are given as mean \pm s.e.m; individual points are also shown for bars.

Figure 4



Anatomical disruption of the nigrostriatal dopaminergic pathway induced by AAV-mediated Cre expression in the SN. (A) AAV-mediated Cre expression in the SN strongly decreased the number of neurons in the SN compacta (SNc) and reticulata (SNr) of *PMAT^{fl/fl}* mice (n=9 per group) and WT mice (n=6 per group), labeled respectively by tyrosine hydroxylase (TH) and parvalbumin (PV) immunofluorescence (n=6-18 SN injections per group). AAV-eGFP-Cre were tested at two concentrations, 3×10^9 genome copies/0.3 μ L (C1) and 2×10^9 genome copies/0.6 μ L (C2). Mann-Whitney test, unpaired, *** p<0.0001. Representative images are shown on the left. Scale bars represent 100 μ m. (B) AAV-mediated Cre expression in the SN of *PMAT^{fl/fl}* mice (n=9 per group) and WT mice (n=6 per group) reduced dopamine transporter (DAT) immunofluorescence in dorsal striata of *PMAT^{fl/fl}* mice (n=9 SN injections per group) and WT mice (n=6 SN injections per group). Intensity is expressed as percentage of mean values for AAV-eGFP controls. DLS, dorsolateral striatum; DMS, dorsomedial striatum. Student t-test, unpaired, ** p<0.01, *** p<0.001. Representative images are shown on the left. Scale bars represent 500 μ m. Values are given as mean \pm s.e.m; individual points are also shown for bars.

Figure 5



Increase in DNA break and programmed cell death markers induced by AAV-mediated Cre expression in the SN. (A-B) AAV-mediated Cre expression in WT mice (n=6 mice per group) increased the number of cells positive for S439 phosphorylated H2AX (A; n=12 SN injections per group) and for K283 acetylated p53 (B; n=8-9 SN injections per group) in the SN of WT mice. Inset in A shows higher magnification of S439 phosphorylated H2AX apoptotic rings in AAV-eGFP-Cre injected mice. Scale bars represent 50 μ m. Student's t-test, unpaired, *** p<0.001. (C) AAV-mediated Cre expression did not alter labeling for D175-cleaved caspase 3 (Cas3), in the SN of WT mice (top; n=6 mice per group). As an internal control, D175-cleaved Cas3 labeling was visible at the level of the scar of injection in the cortex in AAV-eGFP-Cre injected WT mice (bottom). Autofluorescent inclusions were observed in AAV-eGFP-Cre mice. Scale bars represent 50 μ m. (D) AAV-mediated Cre expression induced enlarged cathepsin D labeling in the SN of WT mice (n=6 mice and n=12 SN injections per group) and decreased LC3 labeling in eGFP-expressing cells in SN (n=6 mice and n=6 SN injections per group). Student's t-test, unpaired, *** p<0.001. Scale bars represent 25 μ m for cathepsin D and 50 μ m for LC3. Values are given as mean \pm s.e.m; individual points are also shown for bars.